Radial viscous fingering: Wetting film effects on pattern-forming mechanisms

Pedro H. A. Anjos and José A. Miranda*
Departamento de Física, Universidade Federal de Pernambuco, Recife, Pernambuco 50670-901, Brazil
(Received 27 August 2013; published 6 November 2013)

We consider the interfacial motion between two immiscible viscous fluids in the confined geometry of a radial Hele-Shaw cell. In this framework, we investigate the influence of a thin wetting film trailing behind the displaced fluid on the linear and weakly nonlinear dynamics of the system. More specifically, we examine how the interface instability and the pattern formation mechanisms of finger tip splitting and finger competition are affected by the presence of such a film in the low capillary number limit. Our theoretical analysis is carried out by employing a mode-coupling theory, which allows analytic assess to wetting-induced changes in pattern morphology at the onset of nonlinearities.

DOI: 10.1103/PhysRevE.88.053003 PACS number(s): 47.15.gp, 47.54.−r, 47.20.Ma, 68.08.Bc

I. INTRODUCTION

The viscous fingering (Saffman-Taylor) problem [1] has been extensively studied during the past fifty years or so [2]. It comes about in the narrow passage between two close parallel plates of a Hele-Shaw cell, when a low viscosity fluid displaces a more viscous one. Under such circumstances, an instability develops at the fluid-fluid interface leading to the growth of fingerlike shapes. In the channel geometry of a rectangular Hele-Shaw cell [1,3–5] long, smooth steady state fingers are formed. On the other hand, in radial Hele-Shaw cells [6–8], where the less viscous fluid is injected at the center and drives radially the more viscous fluid, the emerging fingering structures compete and continue to evolve through repeated tip splitting. In this scenario new fingers are continuously generated, eventually resulting in a densely branched interfacial pattern [9,10]. Finger tip splitting and finger competition are the basic nonlinear mechanisms of the viscous fingering process.

Although highly nonlinear, due to its relative simplicity the viscous fingering instability has become a prototypical free boundary problem for many pattern-forming systems of both practical and academic relevance. The dynamic evolution of the problem is governed by the Hele-Shaw flow equations, described by a quasi-two-dimensional, gap-averaged Darcy's law (essentially fluid velocity proportional to the negative of the pressure gradient) and fluid incompressibility (divergenceless velocity field), supplemented by two boundary conditions at the interface [1–10]: a pressure jump as given by a Young-Laplace equation and the continuity (kinematic) condition for the normal component of the fluid velocity.

Despite the usefulness and effectiveness of the simplest version of the Hele-Shaw flow equations in describing critical issues such as interface stability, its original formulation has been improved over the years in order to provide a better match between theory and experiments. One particularly important improvement refers to the incorporation of three-dimensional effects related to the curvature in the transverse direction to the cell plates, as well as to the influence of wall wetting effects [11–20]. One major issue investigated in these works is the fact that the displaced viscous fluid wets the cell walls, leaving a film of finite thickness behind. In particular, Park and Homsy [12] have shown that, in the limit of low capillary number Ca (relative measure of viscous and interfacial tension forces), the inclusion of the effects due to the thin wetting film leads to an order $Ca^{2/3}$ correction to the pressure difference boundary condition.

In fact, comparison between theory [12,16,17] and experiments [13,14] in rectangular Hele-Shaw cells revealed that the addition of the thin wetting film correction into the Young-Laplace condition is indeed necessary to provide a more satisfactory agreement between theoretical and experimental results. These findings reinforced the theoretical claim that the effect of the film has an important influence on the fingering dynamics in Hele-Shaw flows.

Curiously the great majority of studies dealing with the effects of thin wetting films focus on flows occurring in rectangular Hele-Shaw cells [11–17]. There are some studies addressing wetting film effects in radial Hele-Shaw flows, but in the context of centrifugally driven flows in a rotating Hele-Shaw cell [18,21,22]. Experiments performed in dry and prewetted rotating Hele-Shaw cells investigated the stable [21] and unstable [22] displacements of a rotating fluid annulus and have demonstrated that the stability of the annular structure depends substantially on the wetting conditions at the leading interface. Further experimental and numerical studies have been performed in Ref. [18], which considered the relevance of wetting in viscous fingering patterns arising on the border of a dense fluid droplet in a rotating Hele-Shaw cell. Their fully nonlinear numerical simulations and experiments have detected interface stabilization due to dynamic wetting.

In addition to the studies mentioned in the previous paragraph, only a few other investigations examined wetting film-related issues for injection-driven flow in radial Hele-Shaw cells. In 1989 Maxworhty [23] contrasted a series of meticulous experiments with various theoretical predictions and found that inclusion of wetting effects improves the agreement between theory and experiments. More recently a theoretical study performed by Kim *et al.* [24] revisited Maxworthy's experimental findings [23], and achieved a better agreement with experiments by taking into consideration the role played by viscous normal stresses [25,26]. Another recent experimental investigation [27] performed measurements of wetting film thicknesses in a radial Hele-Shaw cell.

*jme@df.ufpe.br

 ©2013 American Physical Society

Only very recently a couple of groups carried out linear stability analyses specifically on the topic of film wetting effects on injection-driven radial Hele-Shaw flows [19,20]. In Ref. [19] the wetting film effects on the interface stability are not really discussed, but the calculation leading to their (somewhat cumbersome) linear dispersion relation [their Eq. (3.24)] does include the wetting film correction. The authors of Ref. [20] managed to derive a much simpler expression for the linear growth rate [Eq. (2) in their paper] and actually have shown that the wetting film effects have a stabilizing role, tending to decrease the magnitude of the growth rate of interfacial disturbances at the linear level. This last result is consistent with the rotating Hele-Shaw cell findings of Ref. [18] and with early studies in rectangular cell geometry [14].

It should be emphasized that investigations performed in Refs. [19,20] are restricted to the early time, purely linear regime in injection-driven radial Hele-Shaw flows, so that they cannot assess the effects of film wetting on the fundamental nonlinear mechanisms of finger tip splitting and finger competition. Therefore, a systematic study of the influence of the wetting film on the most salient morphological features of the patterns arising in injection-driven radial Hele-Shaw flows is still lacking. The investigation of these key issues is the main purpose of this work.

The remainder of this paper is structured as follows. Section II presents our theoretical weakly nonlinear approach. From the Hele-Shaw equations including wetting corrections, and under low capillary number conditions, we derive a second-order mode-coupling equation that describes the time evolution of the interfacial amplitudes under injection-driven radial Hele-Shaw flow circumstances. Our analytical mode-coupling theory provides important insights into pattern formation processes at the onset of nonlinear effects, just by considering the interplay between small number of perturbative Fourier modes. In Sec. III we focus on discussing the role played by the wetting thin film in regulating finger tip-splitting phenomena and in determining the behavior of finger competition events. Our concluding remarks are presented in Sec. IV.

II. WEAKLY NONLINEAR APPROACH

Consider a Hele-Shaw cell of gap spacing b containing two immiscible, incompressible, viscous fluids (see Fig. 1). Denote the viscosities of the inner and outer fluids, respectively, as η_1 and η_2. Between the two fluids there exists a surface tension σ. Fluid 1 is injected into fluid 2 at a constant injection rate Q (equal to the area covered per unit time). As in Refs. [11–17,19,20] our weakly nonlinear theory is developed with the assumption that the displaced fluid (fluid 2) wets the walls of the Hele-Shaw cell, leaving behind a thin wetting film. Likewise, it is assumed that the capillary number is small.

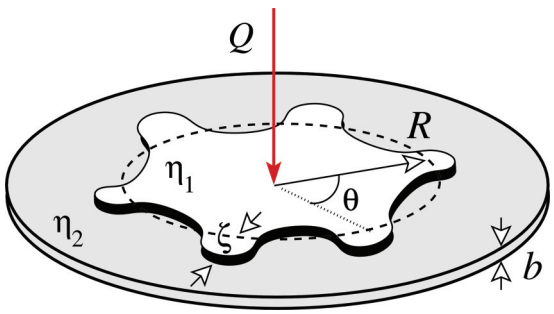

FIG. 1. (Color online) Representative sketch of the injection-driven flow in a radial Hele-Shaw cell.

The perturbed fluid-fluid interface is described as $\Re(\theta,t) = R(t) + \zeta(\theta,t)$, where θ represents the azimuthal angle, and $R(t)$ is the time-dependent unperturbed radius $R = R(t) = \sqrt{R_0^2 + Qt/\pi}$, with R_0 being the unperturbed radius at $t = 0$. Here $\zeta(\theta,t) = \sum_{n=-\infty}^{+\infty} \zeta_n(t)\exp(in\theta)$ denotes the net interface perturbation with Fourier amplitudes $\zeta_n(t)$, and discrete wave numbers n. Our perturbative approach keeps terms up to the second order in ζ. In the Fourier expansion of ζ we include the $n = 0$ mode to maintain the area of the perturbed shape independent of the perturbation ζ. Mass conservation imposes that the zeroth mode is written in terms of the other modes as $\zeta_0 = -(1/2R)\sum_{n\neq 0}|\zeta_n(t)|^2$.

For the effectively two-dimensional geometry of the radial Hele-Shaw cell, the governing equation of the system is the gap-averaged Darcy's law [1,2]

$$\mathbf{v}_j = -\frac{b^2}{12\eta_j}\nabla p_j, \tag{1}$$

where $\mathbf{v}_j$ and p_j denote the velocity and pressure in fluids $j = 1,2$, respectively. From the irrotational nature of the flow ($\nabla \times \mathbf{v}_j = 0$) and the incompressibility condition

$$\nabla \cdot \mathbf{v}_j = 0, \tag{2}$$

it can be readily verified that the velocity potential ϕ_j ($\mathbf{v}_j = -\nabla\phi_j$) obeys the Laplace equation. It this context, to get the equation of motion for the interface, we rewrite (1) for each of the fluids in terms of the velocity potential. Integrate and then subtract the resulting equations from each other to obtain [5,8]

$$A\left(\frac{\phi_1+\phi_2}{2}\right) - \left(\frac{\phi_1-\phi_2}{2}\right) = -\frac{b^2(p_1-p_2)}{12(\eta_1+\eta_2)}, \tag{3}$$

where the dimensionless parameter $A = (\eta_2-\eta_1)/(\eta_2+\eta_1)$ is the viscosity contrast.

To include the contributions coming from surface tension and wetting effects we consider a generalized Young-Laplace pressure boundary condition, which expresses the pressure jump across the fluid-fluid interface [11–20]

$$p_1 - p_2 = -\frac{\pi}{4}\sigma\kappa - \frac{2\sigma}{b}[\cos\theta_c + J\mathrm{Ca}^{\gamma}]. \tag{4}$$

The first term on the right-hand side (RHS) of Eq. (4) represents the contribution related to surface tension and the interfacial curvature κ in the plane of the Hele-Shaw cell. The factor $\pi/4$ is purely a capillary static effect, coming from the z average of the mean interfacial curvature. The second term on the RHS of Eq. (4) accounts for the contribution of the constant curvature associated with the interface profile in the direction perpendicular to the Hele-Shaw cell plates, set by the static contact angle θ_c measured between the plates and the curved meniscus. As in most experiments and wetting models, we consider a nonwetting fluid displacing a wetting one, so that $\theta_c = 0$. Finally, the third term on the RHS of (4) considers the effect of a thin wetting film trailing behind the displaced fluid,

where $\mathrm{Ca} = \eta_2 v_n/\sigma$ is the capillary number, v_n the normal component of the interface velocity, $J = 3.8$, and $\gamma = 2/3$.

At this point, we comment on a noteworthy issue involving the pressure boundary condition (4): Unlike the rectangular Hele-Shaw cell situation [11–17] for which the thickness of the wetting film is constant for a prescribed injection rate, the film thickness could change in the viscous fingering problem in radial Hele-Shaw cells. If one considers that the wetting film thickness scales as the capillary number, which is defined by the finger tip velocity $dR/dt = Q/2\pi R$ (due to mass conservation), the film thickness would decrease in the radial direction. In this scenario the wetting film effect on fingering instability could become less and less pronounced at later times. However, despite this decrease in the wetting film thickness, the fact is that at the onset of nonlinearities (situation treated in this work) we find that wetting film effects are still sizable and do affect the viscous fingering pattern-forming mechanisms. The precise influence of the variable thickness of the wetting film on fully nonlinear dynamics of viscous fingering remains an open question. Proper verification of such effects at the advanced time regime would require intensive numerical simulations and laboratory experiments and are beyond the scope of this work.

The problem we study is specified by the generalized pressure jump boundary condition (4), plus the kinematic boundary condition which states that the normal components of each fluid's velocity are continuous at the interface

$$\frac{\partial \Re}{\partial t} = \left(\frac{1}{r^2}\frac{\partial \Re}{\partial \theta}\frac{\partial \phi_i}{\partial \theta}\right) - \left(\frac{\partial \phi_i}{\partial r}\right). \tag{5}$$

Following standard steps performed in previous weakly nonlinear studies for Hele-Shaw flows [5,8], first, we define Fourier expansions for the velocity potentials. Then we express ϕ_j in terms of the perturbation amplitudes ζ_n by considering condition (5). Substituting these relations, and the pressure jump condition Eq. (4) into Eq. (3), always keeping terms up to second order in ζ, and Fourier transforming, we find the equation of motion for the perturbation amplitudes (for $n \neq 0$)

$$\dot{\zeta}_n = \lambda(n)\zeta_n + \sum_{n'\neq 0}\left\{F(n,n')\zeta_{n'}\zeta_{n-n'} + G(n,n')\dot{\zeta}_{n'}\zeta_{n-n'} + H(n)\left[\dot{\zeta}_{n'}\dot{\zeta}_{n-n'} + \frac{Q}{2\pi R^2}\zeta_{n'}\dot{\zeta}_{n-n'}\right]\right\}, \tag{6}$$

where the overdot denotes total time derivative,

$$\lambda(n) = \frac{1}{1+w(n)}\left[\frac{Q}{2\pi R^2}(A|n|-1) - \frac{\pi\sigma b^2(A+1)}{96\eta_2 R^3}|n|(n^2-1)\right], \tag{7}$$

is the linear growth rate, and

$$w(n) = \gamma|n|J\frac{(A+1)}{12}\frac{b}{R}\left(\frac{2\pi R\sigma}{Q\eta_2}\right)^{1-\gamma} \tag{8}$$

is related to the wetting film contribution. Note that considering the fact that $\dot{R} = Q/2\pi R$ one could write $\eta_2\dot{R}/\sigma = \mathrm{Ca}'$ as a local variable capillary number in these expressions. Even though we do consider the establishment of this time-dependent modified capillary number Ca' in our calculation, we do not write our expressions explicitly in terms of Ca', but rather in terms of η_2, $\dot{R}$, and σ.

The second-order mode-coupling terms are given by

$$F(n,n') = \frac{1}{1+w(n)}\left(\frac{|n|}{R}\left\{\frac{QA}{2\pi R^2}\left[\frac{1}{2} - \mathrm{sgn}(nn')\right] - \frac{\pi b^2\sigma}{48(\eta_1+\eta_2)R^3}\left[1 - \frac{n'}{2}(3n'+n)\right]\right\}, - \frac{3Qw(n)}{4\pi R^3}n'(n-n')\right), \tag{9}$$

$$G(n,n') = \frac{1}{1+w(n)}\left\{\frac{1}{R}[A|n|[1-\mathrm{sgn}(nn')]-1] + \frac{w(n)(1-\gamma)}{2R}\right\}, \tag{10}$$

and

$$H(n) = \frac{w(n)}{1+w(n)}\frac{\pi R}{Q}(1-\gamma), \tag{11}$$

where the sgn function equals ± 1 according to the sign of its argument.

The expressions (6)–(11) represent the mode-coupling equations of the viscous fingering problem in a radial Hele-Shaw cell, taking into consideration the contributions from wetting film effects. This set of nonlinear equations opens up the possibility of investigating analytically how the stability and morphology of the evolving fluid-fluid interface respond to the action of thin film wettability.

We have verified that by setting $\gamma = 0$, Eqs. (6)–(11) reproduce the equivalent expressions originally derived in Ref. [8], where the effects of the wetting film are not taken into account. Note that in this limit a proper match with their results is obtained if the extra $\pi/4$ multiplicative factor appearing in the surface tension term in Eq. (4) is replaced by one.

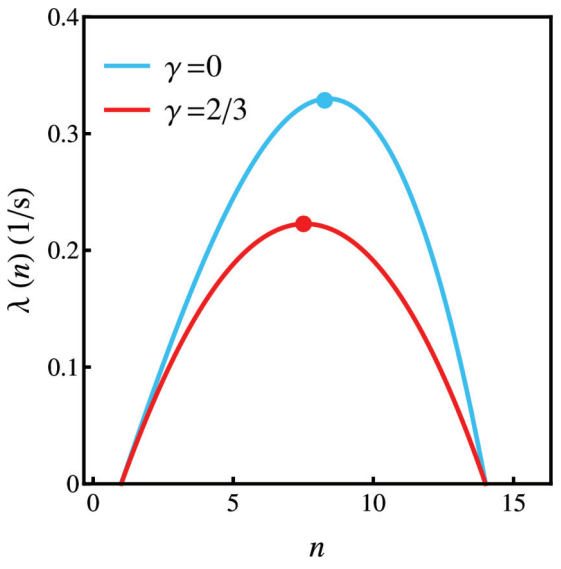

FIG. 2. (Color online) Linear growth rate $\lambda(n)$ as a function of mode n, for the cases without ($\gamma = 0$), and with wetting ($\gamma = 2/3$) at time $t = 6.5$ s. The maxima of the curves are indicated by small dots.

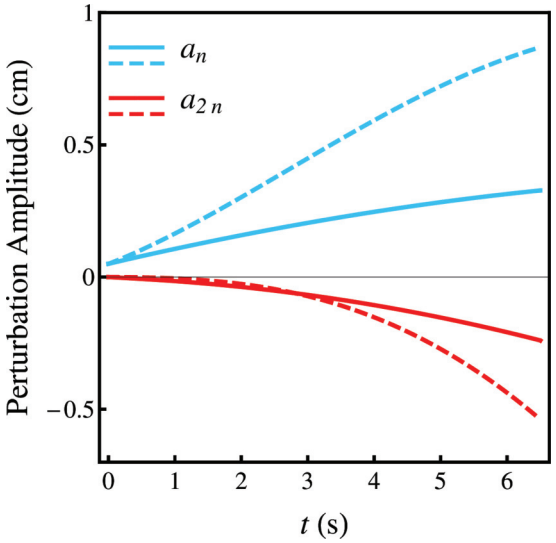

FIG. 3. (Color online) Time evolution of the cosine perturbation amplitudes a_n and a_{2n}. The dashed (solid) curves are plotted for $\gamma = 0$ ($\gamma = 2/3$).

III. WETTING FILM EFFECTS

In the next three subsections we use our mode-coupling approach to investigate the interface evolution at first and second order. To simplify our discussion it is convenient to rewrite the net perturbation in terms of cosine and sine modes

$$\zeta(\theta,t) = \zeta_0 + \sum_{n=1}^{\infty} [a_n(t)\cos(n\theta) + b_n(t)\sin(n\theta)], \qquad (12)$$

where $a_n = \zeta_n + \zeta_{-n}$ and $b_n = i(\zeta_n - \zeta_{-n})$ are real valued. Without loss of generality we may choose the phase of the fundamental mode so that $a_n > 0$ and $b_n = 0$.

We stress that the values we take for our parameters throughout the rest of this work are consistent with typical physical quantities used in real experiments for injection-driven radial viscous flows in Hele-Shaw geometry [2,6,8,9]. Most of the parameters we use are taken from Paterson's classical experiment [6]. We consider the rapid growth of fingers, as air [$\eta_1 \approx 0$] is blown at a constant injection rate $Q = 2\pi$ cm^2/s into glycerin [$\eta_2 \approx 5.21$ g/(cm s)] in a radial source flow Hele-Shaw cell. The thickness of the cell $b = 0.15$ cm and the surface tension $\sigma = 63$ dyne/cm. The initial radius $R_0 = 1.0$ cm and the evolution of the interfaces we consider run up to time $t = 6.5$ s.

A. Linear regime

Although the main focus of our present study is to understand how the wetting film affects intrinsically nonlinear effects related to the morphology of the fingers, for the sake of completeness and clarity we highlight some useful information that can be extracted already at the linear level.

Let us begin by briefly examining Eq. (7): It is interesting to point out that this linear dispersion relation differs from the conventional one (which neglects wetting) just in the prefactor $1/[1 + w(n)]$, which introduces an explicit dependence on γ. So one's first conclusion is that the critical mode n_c of the system, that is, the mode for which $\lambda(n) = 0$, is not modified by the consideration of wetting effects. Therefore, the width of the band of unstable modes [region of Fourier modes within the interval $0 \leqslant n \leqslant n_c$] is not affected by the presence of the wetting fluid. While n_c is not changed, we have verified that the wave number of the fastest growing mode $n_{\max}$ [obtained by setting $d\lambda(n)/dn = 0$] is just slightly reduced when wetting effects are added. Since $n_{\max}$ is connected to the typical number of interfacial fingers rising at the linear level, one anticipates that the number of emerging fingers should not be significantly influenced by the action of wetting. But, if neither n_c nor $n_{\max}$ are strongly affected, one could wonder what would be the main effect of wettability at the linear regime.

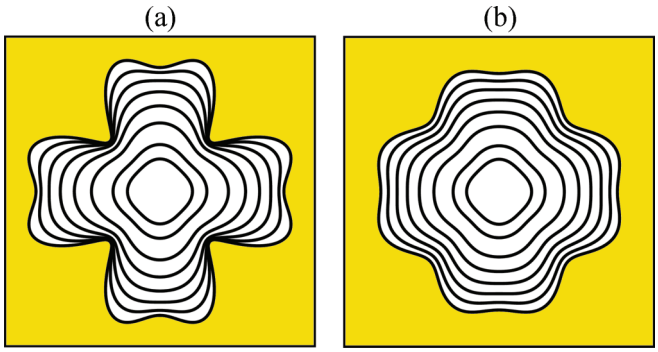

FIG. 4. (Color online) Snapshots of the evolving interface for the interaction of two cosine modes $n = 4$ and $2n = 8$: (a) $\gamma = 0$, and (b) $\gamma = 2/3$.

The answer to this point is given in Fig. 2, which plots the linear growth rate $\lambda(n)$ as a function of mode number n, at time $t = 6.5$ s, for $\gamma = 0$ (wetting is neglected) and $\gamma = 2/3$ (wetting effects are taken into account). It can be seen that even though n_c is kept unchanged, and $n_{\max}$ is just shifted a bit towards lower wave numbers, the magnitude of the growth rate is considerably reduced by the action of wetting. This would indicate that wetting would tend to stabilize the growth of interfacial instabilities at the linear regime. Nevertheless, one must go beyond the purely linear stage in order to explicitly verify how wetting would affect the nonlinear phenomena related to finger tip splitting and finger competition.

B. Weakly nonlinear regime

This section demonstrates the usefulness of our weakly nonlinear analysis in elucidating key aspects related to finger tip behavior and competition under the action of wetting film effects.

1. Tip splitting

At second order the most noteworthy phenomenon in injection-driven radial Hele-Shaw flows is finger tip splitting. Within our mode-coupling approach tip splitting is related to the influence of a fundamental mode n on the growth of its harmonic $2n$ [8]. Under these circumstances, the equations of motion for the cosine and sine modes of the harmonic are

$$\dot{a}_{2n} = \lambda(2n)a_{2n} + \tfrac{1}{2}T(2n,n)a_n^2, \qquad (13)$$

$$\dot{b}_{2n} = \lambda(2n)b_{2n}, \qquad (14)$$

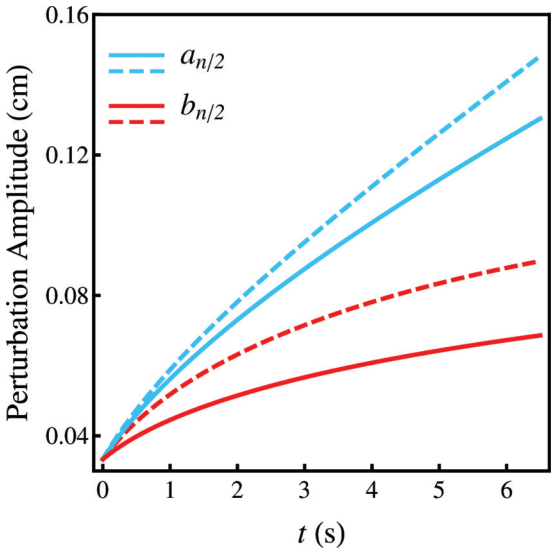

FIG. 5. (Color online) Time evolution of the cosine $a_{n/2}$ and sine $b_{n/2}$ perturbation amplitudes of the subharmonic mode. The dashed (solid) curves are plotted for $\gamma = 0$ ($\gamma = 2/3$).

where

$$T(2n,n) = \Big\{ F(2n,n) + \lambda(n) G(2n,n) + H(2n)\lambda(n)\left[\lambda(n) + \frac{Q}{2\pi R^2}\right]\Big\}. \quad (15)$$

From Eq. (14) we can see that the growth of the sine mode b_{2n} is uninfluenced by a_n, and does not present second-order couplings, so we focus on the growth of the cosine mode. In fact, Eq. (13) shows that the presence of the fundamental mode n forces growth of the harmonic mode $2n$. It has been shown in Ref. [8] that in the absence of wetting film effects a_{2n} is driven negative, precisely the sign that leads to finger tip widening and finger tip splitting. Here we study how the presence of the wetting film could modify this scenario.

To examine the influence of wetting film effects on finger tip behavior at second order, in Fig. 3 we plot the time evolution of the cosine perturbation amplitudes for the fundamental mode (a_n) and for its harmonic mode (a_{2n}). We consider situations in which wetting effects are ignored ($\gamma = 0$, dashed curves) and taken into account ($\gamma = 2/3$, solid curves). We take the initial amplitudes as $a_n = R_0/20$, and $a_{2n} = 0$. By inspecting Fig. 3 it is clear that the presence of wetting does tend to decrease the magnitude of the perturbation amplitudes. Valuable information about finger tip-splitting behavior can be obtained if one focuses on the time evolution for the harmonic mode. When wetting is absent the sign of the harmonic goes strongly negative although its initial value was zero. In this case the nonlinear coupling naturally enhance tendency toward finger tip splitting. However, when wetting effects are considered the magnitude of the harmonic is decreased, indicating that tip splitting would be inhibit. This points to a nonlinear stabilization of the tip-splitting phenomenon induced by the action of the wetting film.

These findings are reinforced and even more clearly illustrated in Fig. 4, which plots the time evolution of the interface for times $t = 0$, 0.5, 1.5, 2.5, 3.5, 4.5, 5.5 and 6.5 s.

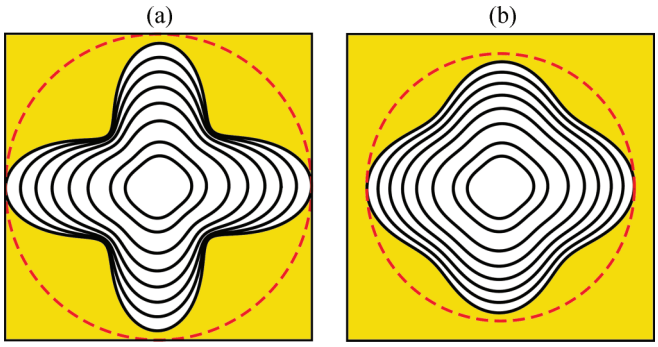

FIG. 6. (Color online) Snapshots of the evolving interface for the interaction of two modes $n = 4$ and $n/2 = 2$ (both sine and cosine) for (a) $\gamma = 0$, and (b) $\gamma = 2/3$. The times shown are the same ones used in Fig. 4. The dashed circle is added to facilitate visualization of finger competition among the outward moving fingers of the inner fluid.

This is done considering the interaction of two cosines modes (a fundamental $n = 4$ and its harmonic $2n = 8$) under the absence (a) and presence (b) of wetting film effects. When wetting is not considered we see typical flowerlike patterns, with the petals presenting tips that clearly split. But, when the wetting film is present, fundamentally different shapes are obtained, and the nonlinear growth of the instability results in the formation of shorter, stubby fingers. In this last case, the usual finger tip-splitting phenomenon is evidently restrained.

2. *Finger competition*

Now we turn our attention to the effects of the wetting film on finger competition events. Once again, we follow Ref. [8] and consider finger length variability as a measure of the competition among fingers. Within our approach the finger competition mechanism can be described by the influence of a fundamental mode n, assuming n is even, on the growth of its subharmonic mode $n/2$. By using Eqs. (6)–(11) the equations of motion for the subharmonic mode can be written as

$$\dot{a}_{n/2} = \{\lambda(n/2) + C(n) a_n\}\, a_{n/2}, \quad (16)$$

$$\dot{b}_{n/2} = \{\lambda(n/2) - C(n) a_n\}\, b_{n/2}, \quad (17)$$

where

$$C(n) = \frac{1}{2}\left[F\left(-\frac{n}{2},\frac{n}{2}\right) + \lambda(n/2) G\left(\frac{n}{2},-\frac{n}{2}\right)\right] + \frac{1}{2}\left[F\left(\frac{n}{2},n\right) + \lambda(n) G\left(\frac{n}{2},n\right)\right] + \frac{1}{2}\lambda(n) H(n/2)\left[\lambda(n/2) + \frac{Q}{2\pi R^2}\right] + \frac{1}{2}\lambda(n/2) H(n/2)\left[\lambda(n) + \frac{Q}{2\pi R^2}\right]. \quad (18)$$

The action of the subharmonic mode breaks the n-fold rotational symmetry of the fundamental by alternately increasing and decreasing the length of each of the n fingers. In Ref. [8] it has been shown that, under injection-driven radial Hele-Shaw flow (without wetting) cosine modes $a_{n/2}$ grow, and sine modes $b_{n/2}$ decay. The result is an increased variability among

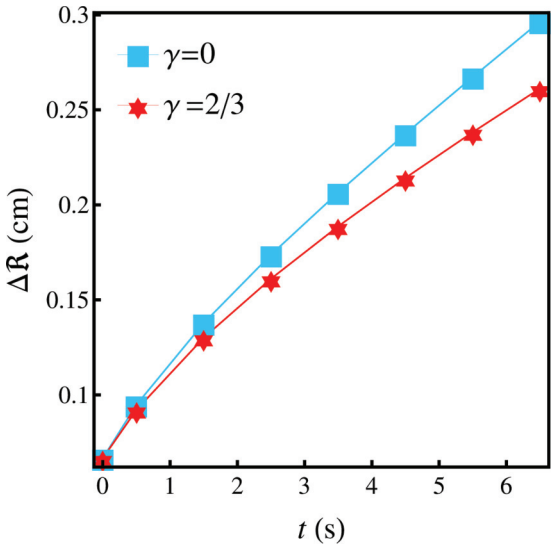

FIG. 7. (Color online) Difference between the interface positions of the finger tips for consecutive outward moving fingers of the inner fluid $\Delta\mathfrak{R}$ as a function of time, for $\gamma = 0$ and $\gamma = 2/3$. This figure uses the same physical parameters utilized in Figs. 5 and 6. It is evident that finger competition is decreased in the presence of wetting effects.

the lengths of the outward moving fingers of the inner fluid invading the outer one. This effect describes the preferential and more intense competition among outward moving fingers.

To get some insight into the effect of wetting on finger competition in Fig. 5 we plot the time evolution of the cosine $a_{n/2}$ and sine $b_{n/2}$ subharmonic amplitudes when wetting effects are ignored ($\gamma = 0$, dashed curves), and taken into account ($\gamma = 2/3$, solid curves). We take the initial amplitudes as $a_{n/2} = b_{n/2} = R_0/30$, and $a_n = R_0/20$. Recall that the finger length variability and the very nature of finger competition depend on the relative magnitudes of sine and cosine subharmonic amplitudes. From Fig. 5 we notice the growth of $a_{n/2}$ over $b_{n/2}$ when $\gamma = 0$. This indicates enhanced competition among the outward moving fingers of the inner fluid, in agreement to what has been obtained in Ref. [8]. When the wetting film effect is considered, one observes that the values of both $a_{n/2}$ and $b_{n/2}$ are lowered (solid curves located below dashed curves), indicating a tendency toward inhibition of finger competition events. We have verified that a similar decrease is detected in the growth of the fundamental mode. These observations indicate that both the size and finger length variability would be decreased as a result of the wetting effects. This is actually what one can see in Fig. 6, where the time evolution of the interface is plotted. If wetting is neglected [Fig. 6(a)] long fingers of different lengths are formed revealing competition among outward moving fingers of the inner fluid. In contrast, short stubby fingers arise when wetting is taken into consideration [Fig. 6(b)].

However, from a purely visual inspection of Figs. 6(a) and 6(b) it is a bit hard to tell for which situation finger competition is most repressed. A clearer illustration of the time evolution of the finger competition behavior in our system is provided by Fig. 7. It plots the difference in finger lengths for consecutive outward moving fingers of the inner fluid $\Delta\mathfrak{R}$ as a function of time, for the times used in Fig. 6. This is done for the cases without ($\gamma = 0$) and with wetting ($\gamma = 2/3$). One can see that finger length variability (i.e., finger competition) changes more significantly with time in the absence of wetting. Therefore, one concludes that finger competition is indeed diminished by the action of the wetting thin film.

IV. CONCLUDING REMARKS

It is well known that wetting film corrections are necessary to provide a more accurate theoretical description of confined flows in rectangular Hele-Shaw cells [11–17]. Interestingly, the studies of the effects of such corrections in the related problem in radial Hele-Shaw cells are scarce, and limited to the purely linear regime [19,20].

In this work we investigated the role played by wetting film corrections on the linear stability and weakly nonlinear dynamics in injection-driven radial Hele-Shaw flows. By employing a mode-coupling approach we have been able to get analytical insight into the changes introduced by wettability on the basic pattern-forming mechanisms of the problem. Our results indicate that the wetting film plays an important role in the overall stabilization of the fingers, restraining the development of both finger bifurcation and finger length variability. We predict the formation of short, stubby fingering structures when the displaced fluid wets the Hele-Shaw walls under radial flow.

ACKNOWLEDGMENTS

We thank CNPq for financial support through the program "Instituto Nacional de Ciência e Tecnologia de Fluidos Complexos (INCT-FCx)" and FACEPE through PRONEM project No. APQ-1415-1.05/10.

[1] P. G. Saffman and G. I. Taylor, Proc. R. Soc. London A **245**, 312 (1958).
[2] For review papers, See G. M. Homsy, Annu. Rev. Fluid Mech. **19**, 271 (1987); K. V. McCloud and J. V. Maher, Phys. Rep. **260**, 139 (1995); J. Casademunt, Chaos **14**, 809 (2004).
[3] G. Tryggvason and H. Aref, J. Fluid Mech. **136**, 1 (1983).
[4] M. W. DiFrancesco and J. V. Maher, Phys. Rev. A **39**, 4709 (1989); **40**, 295 (1989).
[5] J. A. Miranda and M. Widom, Int. J. Mod. Phys. B **12**, 931 (1998).
[6] L. Paterson, J. Fluid Mech. **113**, 513 (1981).
[7] S. S. S. Cardoso and A. W. Woods, J. Fluid Mech. **289**, 351 (1995).
[8] J. A. Miranda and M. Widom, Physica D **120**, 315 (1998).
[9] J.-D. Chen, J. Fluid Mech. **201**, 223 (1989); Exp. Fluids **5**, 363 (1987).

[10] S. W. Li, J. S. Lowengrub, and P. H. Leo, J. Comput. Phys. **225**, 554 (2007).
[11] F. P. Bretherton, J. Fluid Mech. **10**, 166 (1966).
[12] C.-W. Park and G. M. Homsy, J. Fluid Mech. **139**, 291 (1984).
[13] P. Tabeling and A. Libchaber, Phys. Rev. A **33**, 794 (1986).
[14] L. Schwartz, Phys. Fluids **29**, 3086 (1986).
[15] P. G. Saffman, J. Fluid Mech. **173**, 73 (1986).
[16] D. A. Reinelt, Phys. Fluids **30**, 2617 (1987).
[17] D. A. Reinelt, J. Fluid Mech. **183**, 219 (1987).
[18] E. Alvarez-Lacalle, J. Ortín, and J. Casademunt, Phys. Rev. E **74**, 025302(R) (2006).
[19] L. M. Martyushev and A. I. Birzina, J. Phys.: Condens. Matter **20**, 045201 (2008).
[20] E. O. Dias and J. A. Miranda, Phys. Rev. E **88**, 013016 (2013).
[21] Ll. Carrillo, J. Soriano, and J. Ortín, Phys. Fluids **11**, 778 (1999).
[22] Ll. Carrillo, J. Soriano, and J. Ortín, Phys. Fluids **12**, 1685 (2000).
[23] T. Maxworthy, Phys. Rev. A **39**, 5863 (1989).
[24] H. Kim, T. Funada, D. D. Joseph, and G. M. Homsy, Phys. Fluids **21**, 074106 (2009).
[25] E. Alvarez-Lacalle, J. Ortín, and J. Casademunt, Phys. Fluids **16**, 908 (2004).
[26] H. Gadêlha and J. A. Miranda, Phys. Rev. E **79**, 066312 (2009).
[27] T. Ward and A. R. White, Phys. Rev. E **83**, 046316 (2011).